An Attitude Controller for Small Scale Rockets

Florian Kehl, Ankur M. Mehta[1], and Kristofer S. J. Pister

Abstract As technology has advanced, electronic components and systems have become smaller and more powerful. A similar trend holds for space systems, and satellites are no exception. As payloads become smaller, so too can the launch vehicles designed to carry them into orbital trajectories. An energy analysis shows that a rocket system with as low as tens of kg of fuel can be sufficient to deliver a 10g payload into orbit given a sufficiently low mass autonomous rocket flight control system. To develop this, the GINA board, a 2g sensor-laden wireless-enabled microprocessor system, was mounted on a custom actuated rocket system and programmed for inertial flight control. Ground and flight tests demonstrated accurate dead reckoning state estimation along with successful open loop actuator control. Further experiments showed the capabilities of the control system at closed loop feedback control. The results presented in this paper demonstrate the feasibility of a sufficiently low mass flight controller, paving the way for a small scale rocket system to deliver a 10g attosatellite into low Earth orbit (LEO).

1 Introduction

The environment above Earth's atmosphere and beyond is primarily dominated by large one-off spacecraft. Only recently has there been analysis of potential deployments of distributed networks in space (such as in [1–3]). Distributed satellite systems comprising femto- or attosatellites (10-100 grams and 1-10 grams respectively [5]) can enable new atmospheric and astronomical scientific research [6] as well as address wireless sensor network (WSN) research in the absence of notable interference from ground based sources and physical obstacles. As the availablity and functionality of electronics go up and the cost goes down, the required hardware becomes smaller, cheaper, and more accessible. While previous small satellite

UC Berkeley, Berkeley, CA, USA; {kehl,mehtank[1],pister}@eecs.berkeley.edu
[1] Author to whom correspondence should be addressed.

research has focused on systems on the order of kilograms, sensor nodes have shrunk to where a 10 gram system is sufficiently powerful for many purposes.

This paper addresses the issue of deploying such sensor nodes into a low Earth orbit (LEO) for applications in space-based WSNs. In particular, this paper begins to examine a small scale rocket-based solution for delivering a 10 gram attosatellite payload to a desired orbital trajectory. The additional difficulty in miniaturizing a satellite deployment system is offset by the drastically lower cost and risk factors compared to current large-scale launch options.

Ultimately, a launch vehicle (LV) should be of comparable scale and cost to the payload mote being deployed [7]. A full launch solution will also require careful rocket and propellant design; this paper focuses on miniaturizing a control system as described in [8] to be used to guide the LV into a desired trajectory. The hardware developed here is applicable as a final stage in orbital insertion – a rocket was designed and built using low cost, off-the-shelf components to estimate and control system attitude.

An overview of rocket systems and the difficulties in their miniaturization is presented in section 2. The specific hardware designed in this work in described in section 3, with an explanation of the experimental setup and some testing results in section 4. Finally, section 5 offers some conclusions and avenues for future research.

2 Background

2.1 Energy to Low Earth Orbit

Energy considerations drive the mechanical rocket design, constrained by physical properties of available materials.

2.1.1 General rocket equations

A common metric quantifying the energy required to implement an orbital maneuver is the scalar Δv or delta-vee. This energy must be provided by the propulsion system. In the case of a LV moving from rest on the surface of the Earth to LEO, the required Δv_{leo} can be decomposed as follows [9, 10]:

$$\Delta v_{leo} = v_o + \Delta v_d + \Delta v_g + \Delta v_c + \Delta v_{atm} - v_{rot}, \tag{1}$$

where

- v_o is the orbital velocity,
- Δv_d represents the energy lost to drag,
- Δv_g represents the additional gravitational potential energy,
- Δv_c represents energy needed to effect trajectory control,

- Δv_{atm} represents the energy lost due to engine inefficiency in atmosphere,
- v_{rot} is the velocity of the launch platform due to earth's rotation.

The orbital velocity v_o is the speed required to maintain the orbital trajectory. For a circular orbit,

$$v_o = \sqrt{\frac{G \cdot M_e}{(R_e + h)}}, \tag{2}$$

with gravitational constant G, earth's mass M_e and radius R_e, and orbital altitude h. For a satellite in LEO at an altitude of 200 km, this gives $v_o = 7.8$ km/s. The other Δv losses in equation 1 total 1.5 - 2 km/s, yielding a total Δv_{leo} of 9.5 - 10 km/s for a ground launched LV to reach LEO [9].

The total Δv generated by a propulsion system over the duration of a maneuver can be calculated from the time history of its instantaneous thrust ($|F|$) and LV total mass (m):

$$\Delta v = \int_t \frac{|F|}{m} dt. \tag{3}$$

Evaluating this integral for a basic combustion chamber rocket design yields the ideal rocket equation

$$\Delta v = v_e \cdot \ln\left(\frac{m_i}{m_f}\right), \tag{4}$$

where the exhaust velocity v_e is a property of the specific fuel/rocket system.

For a given v_e, then, the Δv of a rocket stage can simply be calculated from that stage's mass ratio m_i/m_f. In practice, the final mass m_f after burnout consists of the structural mass of the rocket along with the payload (which includes higher stages), while the initial mass m_i also includes the mass of the fuel. The total Δv of a multi-stage rocket is the sum of of the Δv's of each stage calculated independently.

2.1.2 Adaptation for minirockets

The drag force experienced by a rocket moving through the atmosphere is given by:

$$F_d = \frac{1}{2}\rho C_d v^2 A, \tag{5}$$

where ρ is the density of the surrounding air, C_d is the drag coefficient, v is the velocity of the rocket relative to the air, and A is the rocket's cross sectional area. This results in a penalty:

$$\Delta v_d = \int \frac{F_d}{m} dt, \tag{6}$$

that scales inversely with length.

As a result, small scale rockets must provide a higher total Δv. Given the ideal rocket equation (4), this means that it is especially important to minimize the mass of the LV, including the electronic flight controller. Thus, the primary specification for the rocket system design becomes the weight metric [11].

The designed rocket system itself need not deliver the total Δv required for orbit. Though a minirocket must still be used to deliver the payload to the specific desired orbital trajectory, some portion of the path can be achieved by bootstrapping on existing aircraft launches. A conventional rocket LV, ultra-high altitude balloon (UHAB), or gun launch system can be used to deploy a system at altitude in the upper atmosphere [12, 13].

There is precedent for such piggyback style systems. The CubeSat program [14] uses spare payload capacity between stages of large scale commercial rocket launches to deploy academic 1 L, 1.33 kg "nano-satellites" into orbit. A UHAB system has been demonstrated to lift a 690 kg payload to a peak altitude of 49.4 km [15], and J.A. Van Allen had used balloons to launch rockets into the upper atmosphere extensively during the 1950s [16].

There are a number of energy advantages for high-altitude launches:

- The gravitational potential energy Δv_g need not be supplied by the rocket.
- The control effort Δv_c is reduced for a shorter trajectory. Not needing to compensate for the wind gusts present at lower altitudes further reduces Δv_c.
- The air drag losses Δv_d experienced by a LV launched above 98.5% of the atmosphere are less than 3% that of a similar system launched from the ground [17].
- The engine operates at peak performance when exhausting into near vacuum, reducing the Δv_{atm} loss caused by to a lower ratio between combustion chamber and ambient pressures [18].

2.1.3 Minirocket design

The design of a complete miniature rocket LEO LV requires a complicated interplay of materials science, aerodynamics, and mechanical engineering [19] – it is a significant undertaking, and beyond the scope of this work. Nonetheless, first order analysis of such a system is necessary to establish the feasibility of such a system.

To keep costs, complexity and structural mass at a minimum, a solid propellant seems to be favorable for a small-scale LV. The need for pipes, valves, tanks, and insulation in liquid propellant engines would contribute to a high overall structural mass. The main disadvantages of solid-fuel propellant are the lower specific impulse I_{sp} and the lack of active throttling, though the latter could potentially be overcome by a combination of intelligent propellant grain design and control system tuning, allowing specific thrust-time characteristics [20].

A solid fuel rocket is little more than an open-ended cylinder packed with fuel (e.g. an ammonium perchlorate oxidizer in a hydroxy-terminated poly-butadiene (HTPB) binder) forming the combustion chamber with a nozzle for exhaust emission, upon which the control system and actuators are mounted. To minimize structural weight, high tensile strength carbon fiber can be used to form the combustion chamber. The physical characteristics of such a system are summarized in table 1.

An single stage to orbit (SSTO) rocket would require that at least 98% of the mass of the rocket be fuel. With required structural mass going to the rocket body, control actuators and electronics, and payload, this requirement proves impossible

Table 1 Physical parameters of a proposed solid fuel minirocket system

Parameter	Subsystem	Value	Units
Fuel exhaust velocity	Fuel	2.6	km/s
Fuel density	Fuel	1.763	g/cc
Chamber pressure	Rocket body	100	atm
Carbon fiber tensile strength	Rocket body	3	GPa
Carbon fiber density	Rocket body	1.75	g/cc
Payload mass	Payload	10	g

or infeasible to satisfy. Instead, staging can be used to distribute the total $\Delta v = 10$ km/s necessary to hit orbit between several stages. This requires a much smaller mass fraction of fuel per stage, bringing the full system down to a manageable size.

2.2 Guidance control system

A rocket LV requires active control for both stability and guidance in order to reach LEO. A typical solid rocket motor is often dynamically unstable, as shown in figure 1. Above atmosphere, passive aerodynamic surfaces cannot provide restoring moments, and so the flight controller must enforce stability. Furthermore, there is no ballistic path to LEO ("what goes up must come down"), so active guidance is necessary to steer the LV along a specified trajectory to reach LEO. Though the lower stages of a multi-stage rocket can be replaced by an alternate carrier as described above, the final, smallest, stage of the minirocket will still need to perform the final orbital trajectory insertion. Thus, it is the design of this controller that is critical to system performance.

Fig. 1 In the absence of aerodynamic forces, a bare solid rocket engine spins out of control. A stabilizing controller is therefore necessary on a minirocket LV.

A schematic of a rocket flight control system is diagrammed in figure 2. In order to implement feedback control, the system must first calculate the state of the LV. In

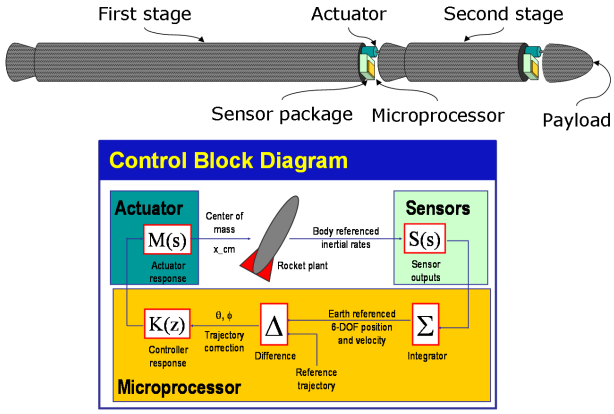

Fig. 2 A feedback control system can be used to stabilize flight and follow a trajectory. The 6DOF state is sensed by a 6 axis IMU and input to a microprocessor. The current heading and trajectory error is calculated, and a control signal is output to an actuator. The actuator positions a mass or aims the nozzle to induce the appropriate torque on the rocket.

principle, an inertial measurement unit (IMU) can measure body-referenced inertial rates, which can be integrated to provide a six degree of freedom (6DOF) state identifying the earth-referenced position and orientation [21]. In practice, additional sensors must also be filtered in to give an accurate state estimate.

Given the state estimate, then, the controller can calculate the deviation from a desired trajectory and command actuators to generate the appropriate corrections. With the final orbital insertion needing to happen above earth's atmosphere, aerodynamic control surfaces such as fins cannot be used. Instead, actuators must direct the body-referenced rocket thrust. These could take the form of a gimbaled nozzle, vanes in the exhaust stream, or an offset mass to generate the required torques for attitude control.

3 Hardware Setup

3.1 Rocket

In order to test the guidance hardware designed for small scale LVs, a model rocket based test system was developed. Miniaturization of this rocket wasn't attempted, as the focus was on the guidance subsystem comprising sensors and actuators.

Off-the-shelf model rocket components were used for the basic rocket structure, namely cardboard tubes, polystyrene and balsa wood. As usual in model rocketry, the rocket contained a parachute for recovery and held disposable off-the-shelf solid-fuel engines. Depending on the experimental setup, different engines with characteristic performances could be mounted. The rocket was designed to carry

the sensors and controller in its body, and incorporated actuators for active control. A camera was also mounted for in-flight video recording for post-flight analysis.

The dimension of the final rocket, shown in figure 3 was 1.25m with a diameter of 0.06m and overall mass of 0.57kg.

Fig. 3 Final rocket: 1) gimbaled nozzle, 2) parachute bay, 3) camera, 4) IMU, motor and payload section, 5) antenna.

3.2 Actuators

To control the longitudinal roll axis (Fig. 4a) , the rocket body (1) contained two concentrically mounted discs (3), driven by two counter-rotating brushless DC motors (2). Controlled acceleration and deceleration of these discs was used to counteract external torques on the rocket's roll axis by compensating angular momentum.

For yaw and pitch control, a gimbaled nozzle was developed to vector the thrust along both axes (Fig. 4b) similar to existing large scale and sounding rockets. An inner engine mount tube (4) was gimbaled on a spherical bearing (7), driven by two high-torque servos (5,6). Controlling the position of the servos steered the rocket engine to point in any direction within a $\pm 4.5^{\circ}$ cone.

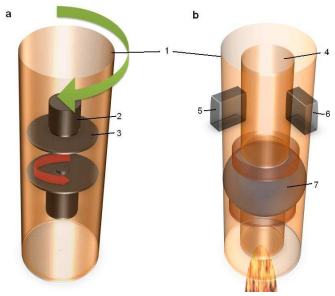

Fig. 4 Control principles: a) spinning discs for roll, b) gimbaled nozzle for pitch and yaw.

3.3 Sensors

An on-board inertial measurement unit (IMU) was used to measure the body referenced 6DOF inertial rates. A MEMS accelerometer measured 3 axis linear motion while MEMS gyros measure the 3 axis angular rates. These sensors can be integrated to calculate the 6DOF position.

However, the outputs of these sensors suffer from additive gaussian noise as well as zero bias drift. The additive noise often integrates out, but the random offset in the rates integrates over time into nontrivial errors. Determining attitude from angular rates requires one integration, and so diverges from true rather slowly; position however is the double integral of acceleration and can accumulate errors rather quickly. To compensate for these errors, additional sensors would be necessary.

Though beyond the scope of this paper, sensors which directly measure position and attitude can be filtered together with the measured rates to generate a more accurate state estimate. Typically, magnetometers, GPS, and cameras complement inertial sensors for localization of robotic systems [22–24]. In the case of minirockets, however, weight is at a premium, and so a minimum of additional sensors are desired. A camera looking at defined features such as the curvature of the earth or celestial bodies can resolve a full 6DOF state estimate, so it may be a good addition to the sensor suite [25].

3.4 Controller

The flight controller for the rocket was a custom designed circuit board for use in small robotic applications, based on the WARPWING project [26]. The Guidance and Inertial Navigation Assistant (GINA) board shown in figure 5 comprises the MEMS inertial sensors, a microcontroller, a 2.4GHz wireless radio, and headers to a daughter card to drive the actuators. The 2g system is the size of a US quarter at half the mass.

Though the microcontroller is capable of implementing control laws itself, for ease of development the system was set up to use a laptop as a command station. The microcontroller polls the sensors and transmits the data wirelessly to a basestation connected to the laptop, which processes the data to generate control outputs. The control signals are send back over the wireless link to the GINA microcontroller, which then drives the actuators via the daughter board. This introduces a slight delay of 6ms in the feedback loop due to time-scheduled communications, as well as a source of errors due to potential packet loss. This cost was tolerated to streamline the development cycle; however a final implementation of an autonomous controller would necessarily incorporate on-board processing to eliminate such problems.

Orbital trajectories are more robust to altitude errors than they are to attitude errors, and so the focus of the controller was on attitude control. The basestation received angular rates from the gyros on the GINA board and integrated them into an attitude estimate. This estimate was demonstrated to track the actual orientation

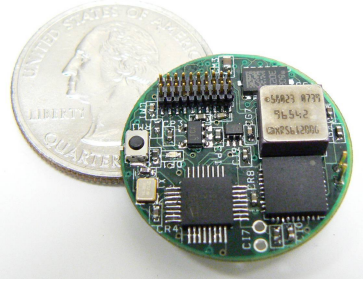

Fig. 5 The 2g GINA controller board incorporates inertial sensing, processing, communications, and actuation. A MEMS accelerometer and gyros, a 2.4 GHz radio, and a connector to an actuator driver board are visible; the processor is on the backside of the board.

of the rocket quite closely over several minutes, and so this state was fed into various feedback loops to control the rocket's roll, pitch, and yaw over the duration of a flight. These loops generated the control signals which were relayed to the GINA board to set the motor speeds and servo positions.

4 Hardware Testing and Experimental Results

4.1 Sensor Validation

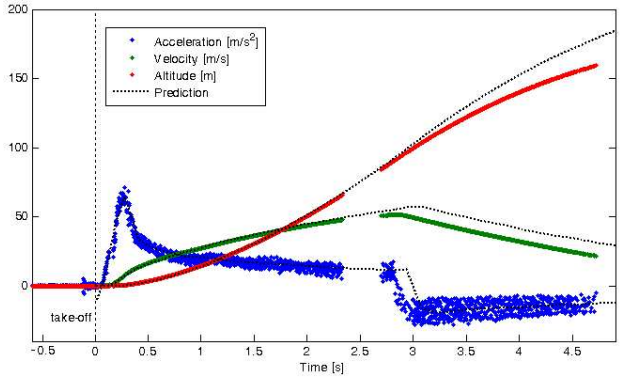

Fig. 6 Measured versus predicted flight profile.

The body-referenced angular rates measured by the IMU can be integrated into a full earth-referenced 6DOF state estimate. Using those measurements, the posi-

tion of a sample uncontrolled rocket flight can be calculated and compared with theoretical predictions. This comparison is shown in figure 6.

The predictions account for aerodynamic drag and gravity and are based on thrust-time data sheets from the National Association of Rocketry NAR for off-the-shelf model rocket engines [27] given the dimensions of the rocket and its time dependent mass. For the latter, we assumed the expelled mass to be proportional to the thrust. Looking at the acceleration, we can clearly see the characteristic thrust-time behavior of the engine (here a *Estes^{TM} E9-4*), with a initial peak thrust due to the engines core burning for the lift-off boost, a subsequent steady burning followed by the engines burnout and deceleration of the rocket during the coasting phase. Predicted and measured data match perfectly until the engine's burnout. A significant shorter burning time of the engine than predicted by the NAR (due to manufacturing tolerances) led therefore to the deviations in velocity and altitude after this event. Around T+2.5s, connection to the basestation was lost for a short period of time due to unknown reason but occurred during a few flights. Tracking the rocket with the antenna decreased the chance of losing data packets.

4.2 Open Loop Actuator Demonstration

4.2.1 Attitude

For safety reasons, the attitude (yaw + pitch) controller was first tested on the ground. The rocket was fixed at its center of gravity, allowing free rotation about the pitch axis (Fig. 7c). Commanding the servo to vector the engine to maximal deflection, +4.5°, led to an angular acceleration of approximately 6rad/s^2 during the peak thrust of a *Estes^{TM} C6-0* engine. This matched quite well with the expected behavior, as seen in figure 7a. The prediction was based on the NAR engine data sheet [27], the thrusting angle and the measured moment of inertia of the rocket. In Fig. 7b, the thrust vector was switched from one endpoint of +4.5° to the opposite endpoint at -4.5° at the time indicated by the vertical dotted line. After about a 0.2s delay caused by accumulated mechanical hysteresis and stiction, the nozzle vectored its thrust in the opposite direction, decelerating the pitching of the rocket, causing it to stop and reverse its rotation.

For the actual open loop controlled flight with the vectored thrust, the rocket was programmed to sinusoidally swing the nozzle in the pitch axis back and forth at a 3 Hz frequency, starting the wiggle when the rocket reached an altitude of 7m. The goal was to directly control the rocket's pitch and hence its trajectory by gimbaling the nozzle. Figure 8b shows the resulting pitch angular velocity. Around T+1s, when the controller's state estimate indicated a 7m altitude, the nozzle started its sinusiodal movement which led to the same wave like pitch movement, revealed by its angular velocity. As seen before, the rocket's response was time shifted by around 0.2s due to stiction and hysteresis. The initial pitching of the rocket is visible on all previous launches, and occurs due to unstable low-velocity behavior. As the relative

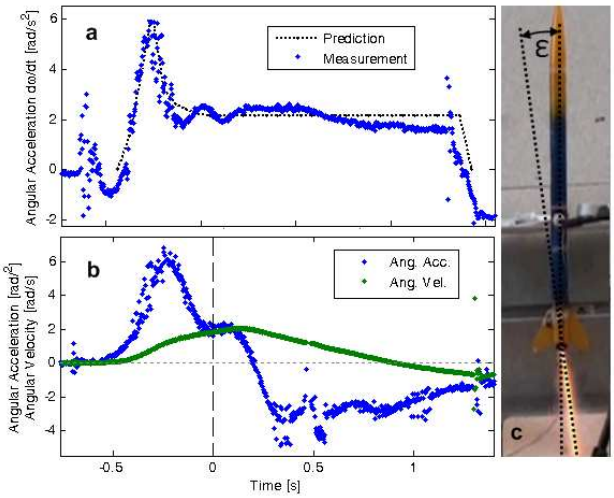

Fig. 7 Angular acceleration depending on thrusting vector ε.

speed of the rocket increases, the fins add stability and the swinging disappears. For this experiment, the rocket was powered by a *Estes*^{TM}*E9-4* engine with a 3s burning time for additional time for thrust vectoring. An evidently wavelike trajectory can be observed in the rocket's smoke trail (Fig. 8a), visually supporting the measured data.

4.2.2 Roll

For roll control, accelerating and decelerating the discs during the flight caused the rocket to rotate back and forth along its longitudinal axis. One big advantage of this system is that it is independent of thrust, being still capable to control during the coasting phase. The major drawback is its tendency for saturation once the motors are spinning at full speed, since the discs act just as a reservoir for angular momentum but are not capable to get rid of it. Knowing expected torques on the rocket body, appropriate disc and motor selection can help to overcome this problem, but might also increase the overall mass.

4.3 Closed Loop Feedback

To keep a rocket on a desired trajectory, closed loop feedback control is necessary. Since the rocket presented in this paper steers by vectoring its thrust in a particular direction, holding the roll axis constant is important to prevent a corkscrew like flight path. Depending on the deviation from the initial roll angle at the launch pad,

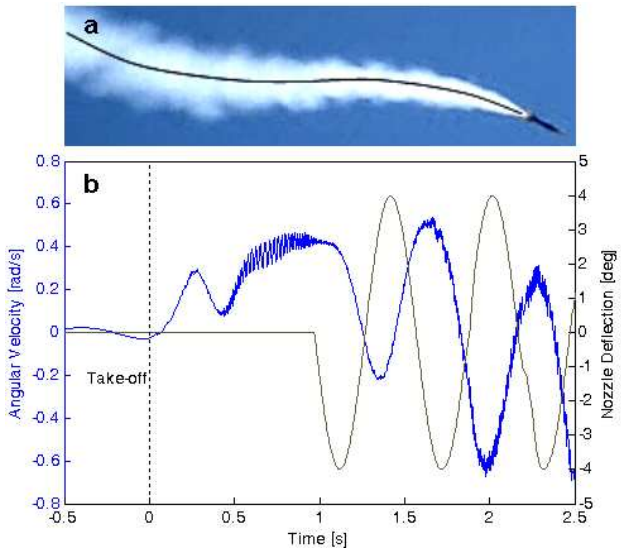

Fig. 8 a) The sinusoidal smoke trail is generated by thrust vectoring, b) Measured angular velocity demonstrates the rocket's response to pitch control. The oscillation immediately after the take-off is due to unstable flight at low velocities

a PID controller drives the rotation speed of the two discs, compensating any external torque, e.g. wind gusts or engine nonuniformities. For testing and simulation purposes, the rocket was suspended by attaching a thread to its nose cone for unhindered longitudinal rotation. Once the PID gains were manually tuned, two sets of experiments were conducted: first, a fan blowing asymmetrically on the rocket fins induced a constant torque; second, a table tennis ball hitting one of the fins generated a torque impulse. In both cases, the PID controller tried to hold the rocket in its initial orientation.

As mentioned above, the actuator can only compensate for a certain amount of angular momentum, limited by the motor speed and the combined moment of inertia of the rotor and disc. Therefore, application of a constant torque will finally end in rotation, but it can be delayed by a significant amount of time as shown on the left in figure 9 compared to the uncontrolled case.

In the case of an abrupt event like the table tennis ball hitting a fin (simulating a short duration gust or the like) the system reacts fast to stop the rotation. In the uncontrolled case (Fig. 9a), the rocket keeps turning steadily after the impact, slightly decelerated by the air resistance of the fins. By contrast, in the PID controlled scenario, the rotation stops suddenly and the roll controller drives the rocket back towards its initial position, as seen in figure 9b. The observed oscillations are vibrations generated by off-center mounting of the reaction masses on the flywheels. Tighter tolerances during manufacturing could improve the respsonse.

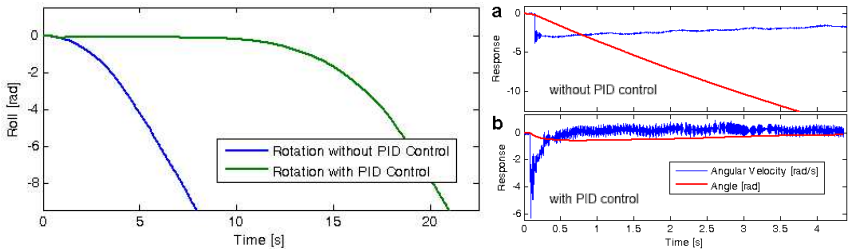

Fig. 9 Roll control with spinning flywheels given constant torque (left) and an impulse (right).

5 Conclusions and Future Work

The experiments presented in this paper demonstrated the validity of delivering small scale satellites into low Earth orbit using minirockets. The extremely small 2g GINA controller was accurately able to estimate a portion of the state required for trajectory control and command actuators to control that state. In the end, an extremely low cost, off the shelf rocket system was demonstrated with the capability for attitude controlled flight.

However, attitude alone is insufficient for orbital insertion, and for longer duration flights additional sensing and sensor fusion are required to compensate for IMU sensor drift. For example, direct state estimates can be generated with a millimeter/milligram scale horizon or star camera, measuring the relative position of the sensor with respect to the earth and/or astronomical bodies. Future work will address these concerns to develop a more robust controller to accurately guide the rocket along longer and more precise trajectories.

Alternate actuation schemes must be also investigated. Though the system presented in this work was able to achieve full attitude control, the actuators and structure required to do so proved to be quite heavy. Reducing the mass of the controllers directly lowers the final system size, and so more efficient ways of effecting stability and guidance control will be necessary. Such actuation could include inserting controllable vanes to deflect the exhaust stream or shifting the position of the payload to adjust the relative thrust vector of the engine.

With a robust, lightweight, and accurate stability and guidance solution for small rocket control, personal scale satellite launches become possible, opening up new avenues of research for scientists and engineers across a wide range of fields.

Supplemental Media

A video showing key features of this work can be seen at:
`http://people.csail.mit.edu/mehtank/minirocketry.mp4`

References

1. Darren L Hitt et al. Mems-based satellite micropropulsion via catalyzed hydrogen peroxide decomposition. *Smart Materials and Structures*, 10(6):1163–1175, 2001.
2. T. Vladimirova et al. Characterising wireless sensor motes for space applications. In *Second NASA/ESA Conference on Adaptive Hardware and Systems*, pages 43–50, August 2007.
3. David J. Barnhart et al. A low-cost femtosatellite to enable distributed space missions. *Acta Astronautica*, 64(11):1123 – 1143, 2009.
4. Siegfried Janson. *Micro/Nanotechnology for Micro/Nano/Picosatellites*. SPACE Conferences & Exposition. American Institute of Aeronautics and Astronautics, September 2003.
5. Herbert J. Kramer and Arthur P. Cracknell. An overview of small satellites in remote sensing. *International Journal of Remote Sensing*, 29(15):4285–4337, 2008.
6. Esteve Bardolet Santacreu. Study of a low cost inertial platfom for a femto-satellite deployed by a mini-launcher. 2010.
7. James R Wertz. *Spacecraft attitude determination and control*, volume 73. Springer, 1978.
8. N. Sarigul-Klijn et al. Air launching earth-to-orbit vehicles: Delta V gains from launch conditions and vehicle aerodynamics. In *42nd AIAA Aero. Sci. Mtg. and Exhibit*, January 2004.
9. Frank J Malina. The problem of escape from the earth by rocket. *Journal of the Aeronautical Sciences (Institute of the Aeronautical Sciences)*, 14(8), 2012.
10. John Tsohas et al. Sounding rocket technology demonstration for small satellite launch vehicle project. In *AIAA 4th Responsive Space Conference. Los Angeles, CA*, pages 1–15, 2006.
11. ED Ransone and DD Gregory. An overview of the NASA sounding rockets and balloon programs. In *17th ESA Symposium on European Rocket and Balloon Programmes and Related Research*, volume 590, pages 19–24, 2005.
12. Valery Kanevsky and Oleg Ventskovsky. Gun launch system for small satellites: A fresh look. In *Small Satellites for Earth Observation: Selected Proc. of the 5th Int'l. Symp. of the Int'l. Academy of Astronautics, Berlin, April 4-8 2005*, page 214, 2005.
13. A. Toorian, K. Diaz, and S. Lee. The cubesat approach to space access. In *Aerospace Conference, 2008 IEEE*, pages 1–14, 2008.
14. E.L. Rainwater and M.S Smith. Ultra high altitude balloons for medium-to-large payloads. In *Advances in Space Research*, volume 33, pages 1648–1652, 2004.
15. J. A. Van Allen. *Balloon-Launched Rockets for High-Altitude Research*, chapter 9. 1959.
16. S.J. Gizinski and J.D. Wanagas. Small satellite delivery using a balloon-based launch system. In *International Communication Satellite Systems Conference and Exhibit*, March 1992.
17. R.A. Nakka. *Solid Propellant Rocket Motor Design and Testing*. U. Manitoba, 1984.
18. Roger Jove-Casulleras, Joshua Tristancho, and Carlos Vera-Flores. *Technical Constraints for a Low-Cost Femto-Satellite Launcher*. AIAA Aero. Sci. Mtg. January 2011.
19. HS Tsien. Optimum thrust programming for a sounding rocket. *Journal of the American Rocket Society*, 21(5):99–107, 1951.
20. Alejandro S Ghersin and Ricardo S Sanchez Pena. Lpv control of a 6-dof vehicle. *Control Systems Technology, IEEE Transactions on*, 10(6):883–887, 2002.
21. Andrew Mark Eldridge. Improved State Estimation for Miniature Air Vehicles. Master's thesis, Brigham Young University, 2006.
22. Peter Gemeiner, Peter Einramhof, and Markus Vincze. Simultaneous Motion and Structure Estimation by Fusion of Inertial and Vision Data. *The International Journal of Robotics Research*, 26(6):591–605, 2007.
23. Oliver Montenbruck and Markus Markgraf. A gps tracking system with onboard iip prediction for sounding rockets. *Journal of Spacecraft and Rockets*, 41:644–650, 2003.
24. L Izquierdo and J Tristancho. Next generation of sensors for femto-satellites based on commercial-of-the-shelf. In *Digital Avionics Systems Conference (DASC), 2011 IEEE/AIAA 30th*, pages 8A4–1. IEEE, 2011.
25. Ankur M Mehta and Kristofer SJ Pister. Warpwing: A complete open source control platform for miniature robots. In *IROS*, pages 5169–5174. IEEE, 2010.
26. National association of rocketry: NAR certified motors. `http://www.nar.org/SandT/NARenglist.shtml`. (Updated 03 June 2009, accessed 15 Sept. 2009).